

# Hybrid scaling properties of localization transition in a non-Hermitian disorder Aubry-André model

Yue-Mei Sun<sup>1</sup>, Xin-Yu Wang<sup>1</sup>, Zi-Kang Wang<sup>2</sup>, and Liang-Jun Zhai<sup>1\*</sup>

<sup>1</sup>*The school of mathematics and physics, Jiangsu University of Technology, Changzhou 213001, China and*

<sup>2</sup>*School of Physics, Sun Yat-Sen University, Guangzhou 510275, China*

(Dated: June 11, 2024)

In this paper, we study the critical behaviors in the non-Hermitian disorder Aubry-André (DAA) model, and we assume the non-Hermiticity is introduced by the nonreciprocal hopping. We employ the localization length  $\xi$ , the inverse participation ratio (IPR), and the real part of the energy gap between the first excited state and the ground state  $\Delta E$  as the character quantities to describe the critical properties of the localization transition. By performing the scaling analysis, the critical exponents of the non-Hermitian Anderson model and the non-Hermitian DAA model are obtained, and these critical exponents are different from their Hermitian counterparts, indicating the Hermitian and non-Hermitian Anderson and DAA models belong to different universe classes. The critical exponents of non-Hermitian DAA model are remarkably different from both the pure non-Hermitian AA model and the non-Hermitian Anderson model, showing that disorder is an independent relevant direction at the non-Hermitian AA model critical point. We further propose a hybrid scaling theory to describe the critical behavior in the overlapping critical region constituted by the critical regions of non-Hermitian DAA model and the non-Hermitian Anderson localization.

## I. INTRODUCTION

In the process of material preparation and experiment, disordered factors such as impurities and defects are inevitable. In 1958, Anderson proposed the famous Anderson model to investigate the effect of disorder on phases and phase transitions [1]. Theoretically, one dimensional (1D) or 2D Anderson model localize for any infinitesimal disorder amplitude, and in 3D Anderson model the localization transition should emerge at some finitely nonzero disorder amplitude [2, 3]. In addition to disorder, quasiperiodic systems [4–8] that the translational invariance is broken by the incommensurate period can also lead to Anderson localization. Among many theoretical quasiperiodic models, the Aubry-André model (AA) is one of the most celebrated examples [9–21], partly inspired by its realization in the pseudorandom optical lattice [22] and ultracold atoms [23]. A remarkable feature of the AA model is the self-duality, which manifests an energy independent localization transition occurring at finite quasi-periodic potential [24].

Although both disorder and quasi-periodicity can lead to localization transitions, theoretical studies have uncovered significant disparities between the two mechanisms, e.g., the localization-extended transition can happen even in the 1D AA model [9]. Moreover, scaling analysis showed that localization transitions in disorder systems and in quasiperiodic systems belong to two distinct universality classes and present different critical behavior [4, 13, 19, 25–32]. For example, the critical exponents of the 1D AA model and the 1D Anderson model are different [13, 25–27]. For the many-body localization (MBL) in the interacting disorder or quasi-periodic sys-

tems, exact diagonalization and real space renormalization group studies indicated that MBL transitions also can be categorized into different universal classes with their specific critical exponents that depend on symmetry class and dimensionality [19, 30–32]. Recently, Bu et al. have introduced a disorder AA (DAA) model that seamlessly merges the mechanisms of localization into a unified framework [13, 14]. It was shown that disorder and quasi-periodic potentials act as two different relevant directions, and rich critical phenomena in the critical region spanned by the quasi-periodic and disorder potentials was found. In particular, a remarkable characteristic of this model is the presence of an overlapping critical region constructed by the critical regions of DAA model and Anderson localization.

In recent years, there has been a surge in the development of non-Hermitian physics, which has found applications across a broad spectrum of condensed matter physics [33–45]. The interplay between the non-Hermiticity and disorder or quasi-periodic also brings new perspectives to our understanding of localization transition [32, 46–70]. The non-Hermitian extension of Anderson model by Hatano and Nelson, discovered that a mobility edge can indeed form in even 1D [46, 47]. For the non-Hermitian quasi-periodic system, it has been demonstrated that the non-Hermiticity can induce reentrant localization, i.e., the localization transition can appear twice as the strength of the quasi-periodic is increased [68]. For the non-Hermitian AA model with nonreciprocal hopping or gain and loss, it has been observed that the localization transition consistently occurs in tandem with both a topological phase transition and a transition from real to complex of energy spectra [54, 55, 57]. More importantly, the introduction of non-Hermiticity can also significantly alter the critical behavior of localization transitions, e.g., the Hermitian and non-Hermitian AA systems belong to different uni-

---

\*Electronic address: [zhailiangjun@jsut.edu.cn](mailto:zhailiangjun@jsut.edu.cn)

versality classes [25, 66]. However, the impact of non-Hermiticity on the critical behaviors of the DAA model still remains unexplored.

In this paper, we investigate the scaling properties of the localization transition in a non-Hermitian DAA model, and we assume that the non-Hermiticity of this model is introduced by the non-reciprocal hopping. We use the localization length  $\xi$ , the inverse participation ratio (IPR), and the real part of the energy gap between the first excited state and the ground state  $\Delta E$  as character observables to perform our scaling analysis. The scaling functions of these quantities are established, and the critical exponents for the pure non-Hermitian Anderson model and the non-Hermitian DAA model are determined. We find that the exponents of the non-Hermitian DAA model are different from the counterparts for both the non-Hermitian Anderson model and non-Hermitian AA model, indicating that the disorder is an independent relevant direction at the non-Hermitian AA critical point. Our scaling also discover that non-Hermitian DAA model and the Hermitian DAA model belong to different universality classes. Furthermore, the overlapping critical region, constituted by the critical regions of non-Hermitian DAA model and the non-Hermitian Anderson localization transition, is also found for the non-Hermitian DAA model, and a hybrid scaling theory of localization transition in this overlapping critical region is proposed.

The rest of the paper is arranged as follows. The non-Hermitian DAA model and the character observables are introduced in Sec. II. In Sec. III, we perform our scaling analysis on the pure non-Hermitian Anderson model and non-Hermitian DAA model, and determine the critical exponents. Then in Sec. IV, by taking disorder and quasi-periodic potentials as scaling variables, the general finite size scaling forms of these three observables are established and verified. Moreover, a hybrid scaling theory in the overlapping region is also proposed and numerically verified. A summary is given in Sec. V.

## II. THE NON-HERMITIAN DAA MODEL AND THE CHARACTER OBSERVABLES

### A. The non-Hermitian DAA Model

The Hamiltonian of the non-Hermitian DAA model reads

$$H = - \sum_j^L (J_L c_j^\dagger c_{j+1} + J_R c_{j+1}^\dagger c_j) + \Delta \sum_j^L w_j c_j^\dagger c_j + (2J_R + \delta) \sum_j^L \cos[2\pi(\gamma j + \phi)] c_j^\dagger c_j,$$

in which  $c_j^\dagger$  ( $c_j$ ) is the creation (annihilation) operator of the hard-core boson,  $J_L = Je^{-g}$  and  $J_R = Je^g$  are

the asymmetry hopping coefficient,  $w_j \in [-1, 1]$  gives the quenched disorder configuration, and  $\Delta$  measures the disorder strength,  $(2J_R + \delta)$  measures the amplitude of the quasi-periodic potential,  $\gamma$  is an irrational number,  $\phi \in [0, 1)$  is phase of the potential. The periodic boundary condition (PBC) is imposed in the following calculation. To satisfy PBC,  $\gamma$  has to be approximated by a rational number  $F_n/F_{n+1}$  where  $F_{n+1} = L$  and  $F_n$  are the Fibonacci numbers [57, 66].

For the non-Hermitian AA model, i.e.,  $\Delta = 0$  in Eq. (1), previous studies have found that it undergoes a localized-extend phase transition at  $\delta = 0$  [57, 66]. For the non-Hermitian Anderson model, i.e.,  $\delta = -2J_R$  in Eq. (1), its ground state remains localized at any finite values of  $\Delta$ , indicating that the phase transition point is always located at  $\Delta = 0$  [46, 47]. For the non-Hermitian DAA model, we have delineated the phase diagram within the  $\delta$ - $\Delta$  parameter plane under a specified value of  $g$ , as depicted in Fig. 1. When  $\delta > 0$ , the non-Hermitian DAA is in the localized phase. When  $\delta < 0$  and  $\Delta = 0$ , this model returns to non-Hermitian AA model, and all the eigenstates is extended. For the pure 1D non-Hermitian Anderson model, the Anderson transition of the ground state of the occurs at  $\Delta = 0$  when  $L \rightarrow \infty$ , which means infinite disorder will localize the wave function for  $\delta < 0$ .

Around the critical point  $(\delta, \Delta) = (0, 0)$ , the critical region of the non-Hermitian DAA model is spanned by  $\Delta$  and  $\delta$ . For  $\delta < 0$  and infinitesimal  $\Delta$ , there is a critical region for the Anderson localization. As a result, near the critical point of  $(\delta, \Delta) = (0, 0)$  and  $\delta < 0$ , these critical regions inevitably overlap with each other.

In Fig. 2, we present the energy spectrum of the non-Hermitian DAA model. Our findings indicate that the energy spectra predominantly exhibit real values when  $\delta > 0$ , whereas they incorporate imaginary components when  $\delta < 0$ . This suggests that the introduction of disorder disrupts the correspondence between the real-complex transition of the energy spectrum and the localization transition in the non-Hermitian AA model. It can be observed that the characteristics of its energy spectrum are very similar to those of the non-Hermitian AA model [66], indicating that one-dimensional quasi-periodic systems are quite stable under perturbations by disorder [30, 71].

### B. character observables

Here, we employ the  $\xi$ , IPR, and  $\Delta E$  to explorer the scaling law in the critical regions.

In the localized phase, the localization length  $\xi$  for the non-Hermitian system is defined as [25, 66]

$$\xi = \sqrt{\sum_{n>n_c}^L [(n - n_c)^2] P_i}, \quad (2)$$

in which  $P_i$  is the probability of the wavefunction at site

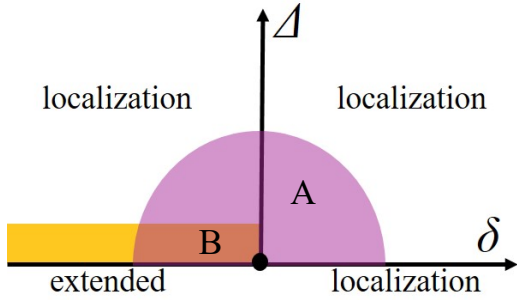


FIG. 1: Sketch of the phase diagram of the non-Hermitian DAA model. The region A (violet region) denotes the critical region of localization transition of the non-Hermitian DAA model. The region B (yellow region) denotes the critical region of the Anderson localization transition. The intersection of regions A and B represents the overlapping critical region where non-Hermitian DAA and non-Hermitian Anderson localization critical regions coexist.

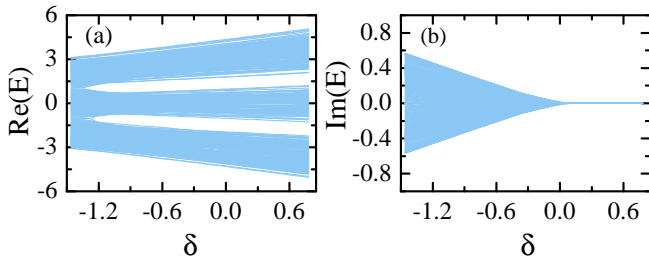


FIG. 2: (a) Real and (b) imaginary parts of energy spectra of the model Eq. (1). The black curves corresponds to the states in which the real spectra for all  $\delta$ 's. Here, we choose  $g = 0.5$ ,  $\phi = 0.2$ ,  $\Delta = 0.8$  and  $L = 377$  in the calculation.

$i$ , and  $n_c \equiv \sum n P_i$  is the localization center. In the thermodynamic limit of  $L \rightarrow \infty$ ,  $\xi$  scales with the distance to the critical point  $\varepsilon$  as

$$\xi \propto \varepsilon^{-\nu}, \quad (3)$$

where  $\nu$  is a critical exponent. For the pure non-Hermitian AA model,  $\varepsilon = \delta$  and  $\nu = \nu_\delta = 1$  under both PBC and open boundary condition (OBC) [66, 72].

IPR is defined as [73, 74]

$$\text{IPR} = \frac{\sum_{j=1}^L \|\Psi(j)\|^4}{\sum_{j=1}^L \|\Psi(j)\|^2}, \quad (4)$$

where  $|\Psi(j)\rangle$  is the right eigenvector. For the extended phase, IPR scales as  $\text{IPR} \propto L^{-1}$ . For the localized state, IPR scales as  $\text{IPR} \propto L^0$ . At the critical point, IPR scales as

$$\text{IPR} \propto L^{-s/\nu}, \quad (5)$$

where  $s$  is a critical exponent. When  $L \rightarrow \infty$ , IPR scales with the distance to the critical point  $\varepsilon$  as

$$\text{IPR} \propto \varepsilon^s. \quad (6)$$

For the non-Hermitian AA model,  $\varepsilon = \delta$  and  $s = s_\delta = 0.1198$  [65, 66].

At the critical point of localization transition, energy gap  $\Delta E$  scales with the lattice size  $L$  as

$$\Delta E \propto L^{-z}, \quad (7)$$

where  $z$  is a critical exponent. For the non-Hermitian AA model,  $\varepsilon = \delta$  and  $z = z_\delta = 2$  [66]. When  $L \rightarrow \infty$ , energy gap  $\Delta E$  scales as

$$\Delta E \propto \varepsilon^{\nu z}. \quad (8)$$

By taking into account of the finite-size effect, the general scaling ansatz of a quantity  $Y$  reads

$$Y(\varepsilon) = L^{y/\nu} f(\varepsilon L^{1/\nu}), \quad (9)$$

where  $y$  is the critical exponent of  $Y$  defined according to  $Y \propto \varepsilon^{-y}$  when  $L \rightarrow \infty$ , and  $f(\cdot)$  is the scaling function.

### III. THE CRITICAL EXPONENTS

In this section, we study the scaling behaviors of the character observables, and obtain the corresponding critical exponents for the pure non-Hermitian Anderson model and the non-Hermitian DAA model.

#### A. The critical exponents for non-Hermitian Anderson model

For the non-Hermitian Anderson model with  $\delta = -2J$  in Eq. (1), the finite-size scaling functions for  $\xi$ , IPR and  $\Delta E$  can be derived from Eqs. (3), (6), (8) and (9). The scaling function for  $\xi$  reads

$$\xi = L f_1(\Delta L^{1/\nu_A}), \quad (10)$$

where  $\nu_A$  is critical exponent for non-Hermitian disorder model, and  $f_i$  is the scaling function. Similarly, the scaling of IPR should satisfy

$$\text{IPR} = L^{-s_A/\nu_A} f_2(\Delta L^{1/\nu_A}), \quad (11)$$

where  $s_A$  is the critical exponent of IPR for non-Hermitian Anderson model. The scaling function for  $\Delta E$  reads

$$\Delta E = L^{-z_A} f_3(\Delta L^{1/\nu_A}), \quad (12)$$

where  $z_A$  is the critical exponent of  $\Delta E$  for non-Hermitian Anderson model.

To determine the critical exponents  $\nu_A$ ,  $s_A$  and  $z_A$ , we numerically calculate these three characterized observables versus disorder strength  $\Delta$ , and rescale according to Eqs. (10) to (12). In Fig. 3 (a1), we plot  $\xi$  versus  $\Delta$  for different  $L$ . After rescaling  $\xi$  and  $\Delta$  as  $\xi L^{-1}$  and  $\Delta L^{1/\nu_A}$  with  $\nu_A = 1.99$ , we find that the rescaled curves collapse

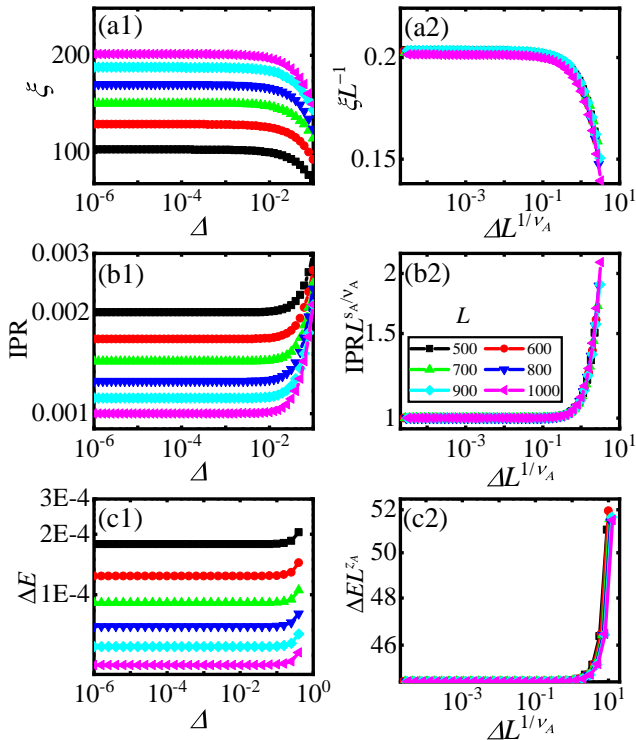


FIG. 3: Scaling properties in the ground state for the pure non-Hermitian Anderson model. The curves of  $\xi$  versus  $\Delta$  before (a1) and after (a2) rescaled for different  $L$ 's. The curves of IPR versus  $\Delta$  before (b1) and after (b2) rescaled for different  $L$ 's. The curves of  $\Delta E$  versus  $\Delta$  before (c1) and after (c2) rescaled for different  $L$ 's. We use  $g = 0.5$ , and the result is averaged for 1000 samples of disorder. The double-logarithmic scales are used.

onto each other very well, as shown in Fig. 3 (a2). In Fig. 3 (b1) and (b2), the numerical results of IPR versus  $\Delta$  before and after rescaling to Eq. (11) are plotted. We find that collapse of the rescaled curves is best when  $s_A = 2$  by setting  $\nu_A = 1.99$  as input. The numerical results of  $\Delta E$  versus  $\Delta$  and the rescaled curves of  $\Delta EL^{z_A}$  versus  $\Delta L^{1/\nu_A}$  are plotted in Fig. 3 (c1) and (c2). By setting  $\nu_A = 1.99$  as input, we find that the best collapse of these rescaled curves appears when  $z_A = 2$ .

Hence, the critical exponent set of the 1D non-Hermitian Anderson model is obtained as  $(\nu, s, z) = (\nu_A, s_A, z_A) = (1.99, 2, 2)$ . It is noteworthy that these critical exponents diverge from those of the 1D Hermitian Anderson model [13, 26], suggesting that non-Hermitian and Hermitian Anderson models are categorized under distinct universality classes.

### B. The critical exponents for the non-Hermitian DAA model

For the non-Hermitian DAA model, the critical exponents along the  $\delta$  and  $\Delta$  directions should be different, since  $\delta$  and  $\Delta$  are two distinct relevant direction. The

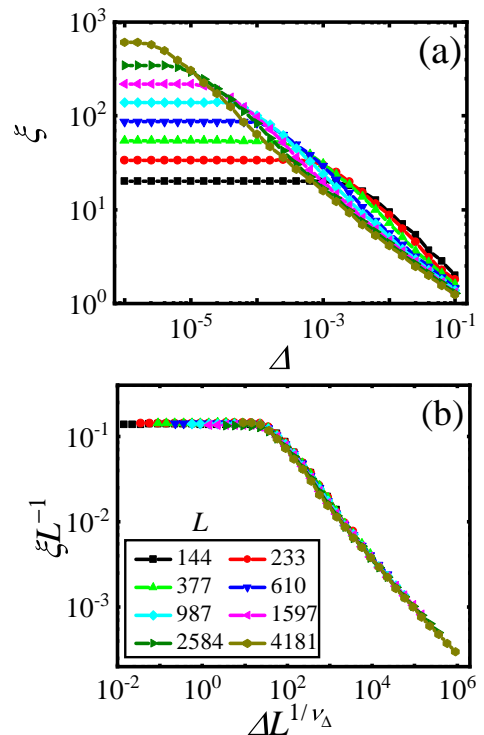


FIG. 4: (a) Curves of  $\xi$  versus  $\Delta$  for the non-Hermitian DAA model at  $\delta = 0$  for various  $L$ 's. (b) The rescaled curves of  $\xi L^{-1}$  versus  $\Delta L^{1/\nu_\Delta}$  according to Eq. (13). We use  $g = 0.5$ , and the result is averaged for 1000 samples. The double-logarithmic scales are used.

non-Hermitian DAA model returns to the non-Hermitian AA model when  $\Delta = 0$ , hence, the critical exponents along the direction of  $\delta$  should be  $(\nu, s, z) = (\nu_\delta, s_\delta, z_\delta) = (1, 0.1198, 2)$  [66]. The scaling exponents along the  $\Delta$  direction  $(\nu, s, z) = (\nu_\Delta, s_\Delta, z_\Delta)$  should be a distinct set from those in the non-Hermitian Anderson model. This is due to the nature of the critical point of  $(\Delta, \delta) = (0, 0)$  being different from the extended state scenario.

Along  $\Delta$  direction, localization length  $\xi$  scales with  $\Delta$  as  $\xi \propto \Delta^{-\nu_\Delta}$ . Similarly, by taking into account of the finite-size effect, the scaling ansatz of  $\xi$  reads

$$\xi = L f_4(\Delta L^{1/\nu_\Delta}). \quad (13)$$

The curves of  $\xi$  versus  $\Delta$  for various  $L$ 's at  $\delta = 0$  are plotted in Fig. 4 (a). After rescaling  $\xi$  and  $\Delta$  according to Eq. (13), we find that the best collapse of these rescaled curves appears when  $\nu_\Delta = 0.52$ , as plotted in Fig. 4 (b). This new critical exponent  $\nu_\Delta$  indicates that the disorder contributes a new relevant direction in the non-Hermitian AA critical point.

From Eq. (7), it is shown that  $\Delta E \propto L^{-z_\delta}$  and  $\Delta E \propto L^{-z_\Delta}$  should be applicable simultaneously, hence, we have  $z_\Delta = z_\delta = 2$ . While for IPR, the simultaneous applicability of Eq. (5) in both directions provides the following relationship

$$s_\Delta = s_\delta \frac{\nu_\Delta}{\nu_\delta}. \quad (14)$$

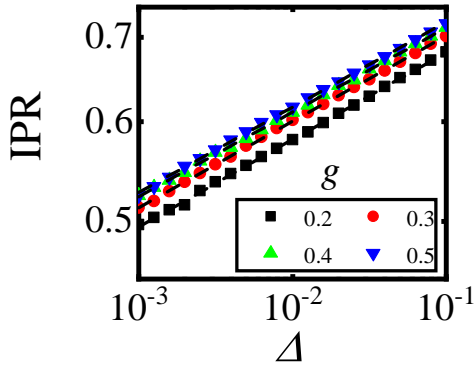


FIG. 5: Curves of IPR versus  $\Delta$  for the non-Hermitian DAA model at  $\delta = 0$  for various  $g$ 's. We use  $L = 4181$ ,  $g = 0.5$  and the result is averaged for 1000 samples. The dashed lines are fitting lines. The double-logarithmic scales are used.

Therefore, along the  $\Delta$  direction,  $\varepsilon = \Delta$  and  $s = s_\Delta$ , Eq. (6) becomes

$$\text{IPR} \propto \Delta^{s_\Delta} = \Delta^{s_\delta \nu_\Delta / \nu_\delta}. \quad (15)$$

By studying the scaling properties of IPR with  $L \rightarrow \infty$ , we can determine  $s_\Delta$  and further verify the critical exponent  $\nu_\Delta$ .

In Fig. 5, IPR versus  $\Delta$  at  $\delta = 0$  for different  $g$  are plotted. The lattice size is  $L = 4181$ , which is large enough so that the size effects are tiny. We find that IPR versus  $\Delta$  are parallel lines in the double-logarithmic coordinates. Notably, the average slope of these lines is  $s_\Delta = 0.0642$ , aligning close to the theoretical prediction value of  $s_\Delta = s_\delta \nu_\Delta / \nu_\delta = 0.0623$  by setting  $\nu_\Delta = 0.52$  as input. This consistency also confirms the correctness of the value of  $\nu_\Delta$ . In addition, since we have calculated the results for different  $g$  and they all fit well with the theoretical predictions, this indicates that the obtained exponent is universally applicable to the non-Hermitian DAA model.

Thus, we obtain the set of critical exponents for the non-Hermitian DAA model in the  $\Delta$  direction as  $(\nu, s, z) = (\nu_\Delta, s_\Delta, z_\Delta) = (0.52, 0.0652, 2)$ . These exponents are different from that of the Hermitian DAA model [13]. This also indicates that non-Hermitian DAA and Hermitian DAA models belong to different universe classes.

#### IV. HYBRID SCALING PROPERTIES AROUND THE CRITICAL POINT OF THE NON-HERMITIAN DAA MODEL

In this section, we study the scaling properties around the critical point of the non-Hermitian DAA model. In particular, a hybrid scaling law is proposed to characterize scaling properties in the overlapping critical region constructed by the non-Hermitian DAA critical region and the Anderson localization transition.

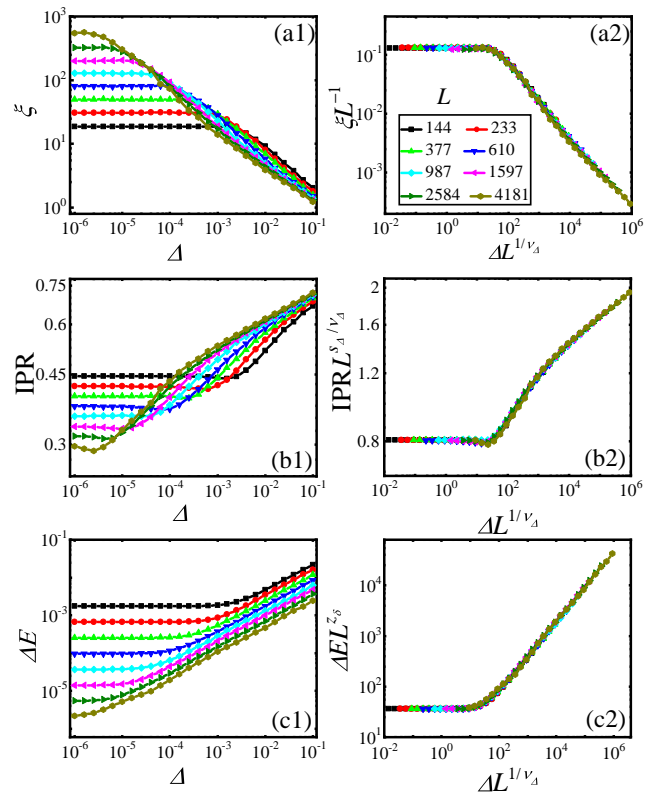


FIG. 6: Scaling properties in the ground state for fixed  $\delta L^{1/\nu_\delta} = 1$ . The curves of  $\xi$  versus  $\Delta$  before (a1) and after (a2) rescaled for different  $L$ 's. The curves of IPR versus  $\Delta$  before (b1) and after (b2) rescaled for different  $L$ 's. The curves of  $\Delta E$  versus  $\Delta$  before (c1) and after (c2) rescaled for different  $L$ 's. Here,  $g = 0.5$ , and the result is averaged for 1000 samples. The double-logarithmic scales are used.

##### A. Full scaling forms in the critical regions

By taking  $\Delta$  and  $\delta$  as scaling variables, the general finite size scaling forms of these three observables are

$$\xi = L f_5(\delta L^{1/\nu_\delta}, \Delta L^{1/\nu_\Delta}), \quad (16)$$

$$\text{IPR} = L^{-s_\delta/\nu_\delta} f_6(\delta L^{1/\nu_\delta}, \Delta L^{1/\nu_\Delta}), \quad (17)$$

$$\Delta = L^{-z_\delta} f_7(\delta L^{1/\nu_\delta}, \Delta L^{1/\nu_\Delta}). \quad (18)$$

In the critical region of the non-Hermitian DAA model, the scaling functions Eqs. (16) to (18) should be applicable.

In the overlapping critical region of  $\delta < 0$ , both the scaling functions of the non-Hermitian Anderson transitions and the non-Hermitian DAA model should play significant roles. Here, to study the scaling behavior in this overlapping critical region, the following hybrid scaling law is proposed. In a typical scenario where the overlapping critical region is postulated to be composed of Critical Region A and Critical Region B, the hybrid scaling laws propose the following hypotheses: First, within the overlapping critical region, the critical properties should be concurrently describable by the critical theories per-

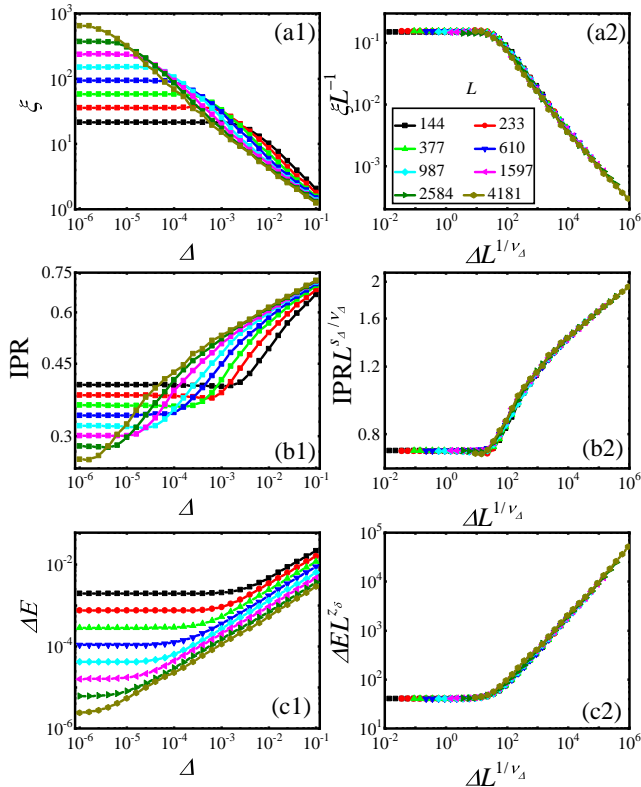


FIG. 7: Scaling properties in the ground state for fixed  $\delta L^{1/\nu_\delta} = -1$ . The curves of  $\xi$  versus  $\Delta$  before (a1) and after (a2) rescaled for different  $L$ 's. The curves of IPR versus  $\Delta$  before (b1) and after (b2) rescaled for different  $L$ 's. The curves of  $\Delta E$  versus  $\Delta$  before (c1) and after (c2) rescaled for different  $L$ 's. Here,  $g = 0.5$ , and the result is averaged for 1000 samples. The double-logarithmic scales are used.

taining to both Region A and Region B. Second, a constraint between the scaling functions of both Region A and Region B should be imposed.

It's worth noting that overlapping critical regions are a common phenomenon in condensed matter physics [13, 75–79], and this hybrid scaling law has a general and universal significance. For instance, both the Hermitian DAA and AA-Stark models exhibit overlapping critical regions of localization transition, and they have also confirmed the correctness of this hybrid scaling law [13, 75]. Similarly, in the study of the non-equilibrium dynamics in the Yang-Lee edge singularity, a hybrid Kibble-Zurek scaling has been proposed to describe the behavior of driven dynamics in overlapping critical regions [76, 77].

Here, we take the critical properties of  $\xi$  to illustrate this hybrid scaling law. According to this hybrid scaling law, both the scaling functions of  $\xi$ , i.e., Eqs. (10) and 16, are applicable in the critical region with  $\delta < 0$ . Combining Eqs. (10) and (16), the constraint between these two scaling functions should satisfy

$$f_5(\delta L^{1/\nu_\delta}, \Delta L^{1/\nu_\Delta}) = f_1[\Delta L^{1/\nu_\Delta} (\delta L^{1/\nu_\delta})^\kappa], \quad (19)$$

where  $\kappa \equiv \nu_\delta(1/\nu_A - 1/\nu_\Delta)$ . We find that  $\kappa$  includes

both the critical exponents of non-Hermitian DAA model and non-Hermitian Anderson model, which gives the constraint between these scaling functions.

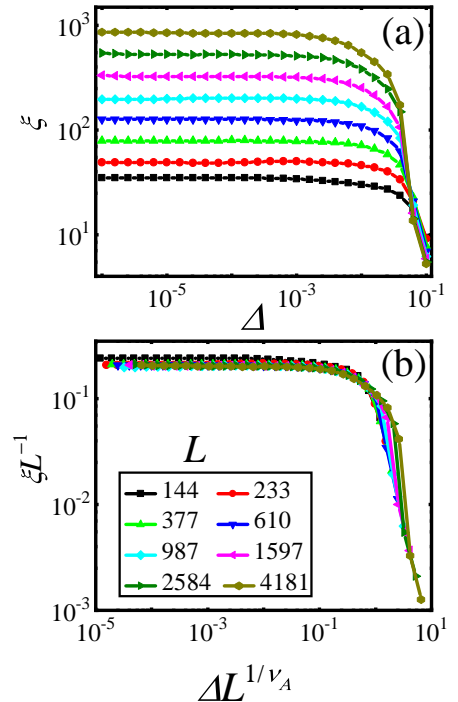


FIG. 8: (a) The curves of  $\xi$  versus  $\Delta$  for different  $L$ 's at  $\delta = -0.5$ . (b) Rescaled curves of  $\xi L^{-1}$  versus  $\Delta L^{1/\nu_A}$  collapse onto each other. Here,  $g = 0.5$ , and the result is averaged for 1000 samples of  $\phi$ . The double-logarithmic scales are used.

## B. Numerical results

In this section, we numerically verify these scaling theories. By fixing  $\delta L^{1/\nu_\delta}$  to constant, Eqs. (16) to (18) are firstly verified. In Figs. 6, the scaling properties of  $\xi$ , IPR and  $\Delta E$  versus  $\Delta$  for  $\delta L^{1/\nu_\delta} = 1$  are plotted. After rescaling according to Eqs. (16) to (18), the rescaled curves collapse onto each other well, confirming Eqs. (16) to (18). In the overlapping critical region with  $\delta < 0$ , the similar numerical results for fixing  $\delta L^{1/\nu_\delta} = -1$  are plotted in Fig. 7. The collapse of the rescaled curves shown in Fig. 7 (a2), (b2) and (c2) also confirms Eqs. (16) to (18).

Then, we take  $\delta = -0.5$  as example to examine the applicability of Eq. (10) in the overlapping region, and the numerical results are plotted in Fig. 8. We find that the rescaled curves collapse onto each other well, indicating that Eqs. (10) is still applicable in this overlapping region. Therefore, numerical results in Figs. 7 (a1) and (a2) and Fig. 8 confirm the first hypothesis of the hybrid scaling laws.

The numerical results of  $f_5 = \xi L^{-1}$  as a function of  $\Delta L^{1/\nu_\Delta}$  for various  $\delta < 0$  are plotted in Fig. 9 (a). By

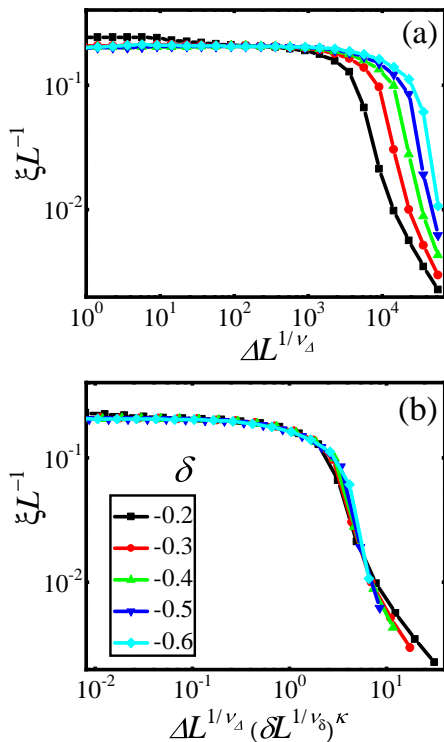


FIG. 9: (The curves of  $\xi L^{-1}$  versus  $\Delta L^{1/\nu_\Delta}$  for different  $\delta$ 's at  $L = 987$ . (b) Rescaled curves of  $\xi L^{-1}$  versus  $\Delta L^{1/\nu_\Delta} (\delta L^{1/\nu_\delta})^\kappa$  collapse onto each other. Here,  $g = 0.5$ , and the result is averaged for 1000 samples. The double-logarithmic scales are used.

rescaling  $\Delta L^{1/\nu_\Delta}$  as  $\Delta L^{1/\nu_\Delta} (\delta L^{1/\nu_\delta})^\kappa$ , we find that the rescaled curves collapse very well, verifying Eq. (19) and the second hypothesis of the hybrid scaling law.

## V. SUMMARY

In summary, we have studied the critical behaviors of the non-Hermitian DAA model with non-Hermiticity be-

ing induced by the non-reciprocal hopping. The scaling functions of these quantities for the non-Hermitian Anderson model, the non-Hermitian DAA model are obtained, and the critical exponents of these models have been determined. We have discovered that the critical exponent of the non-Hermitian DAA are different from the non-Hermitian Anderson model and non-Hermitian AA model, which means the disorder provides a new relevant direction in the non-Hermitian AA critical point. Critical properties in the critical region spanned by the disorder and quasi-periodic potentials are explored in detail. Especially, in the overlapping region constituted by the critical regions of the non-Hermitian DAA model and the non-Hermitian Anderson localization, a hybrid scaling theory is proposed and numerically verified.

On-site gain and loss is another important form of non-Hermiticity, and many studies have shown that the effects of this non-Hermiticity on the localization are quite different from those of non-reciprocal effects [54, 80]. Therefore, as a potential extension of this paper, it is also worth investigating the non-Hermitian DAA with on-site gain and loss. Additionally, since the non-Hermitian disorder or quasi-periodic models are also highly sensitive to boundary conditions [45, 81], it is also necessary to discuss the critical properties of the non-Hermitian DAA model under OBC. This could also be a possible extension of this paper.

## Acknowledgments

This work is supported by the National Natural Science Foundation of China (Grant No. 12274184) and Qing Lan Project.

- 
- [1] P. W. Anderson, Absence of diffusion in certain random lattices, *Phys. Rev.* **109**, 1492 (1958).
  - [2] J. Šuntajs, T. c. v. Prosen, and L. Vidmar, Localization challenges quantum chaos in the finite two-dimensional Anderson model, *Phys. Rev. B* **107**, 064205 (2023).
  - [3] A. Yamilov, S. E. Skipetrov, T. W. Hughes, M. Minkov, Z. Yu, and H. Cao, Anderson localization of electromagnetic waves in three dimensions, *Nat. Phys.* **19**, 1308 (2023).
  - [4] U. Agrawal, S. Gopalakrishnan, and R. Vasseur, Universality and quantum criticality in quasiperiodic spin chains, *Nat. Commun.* **11**, 2225 (2020).
  - [5] V. Goblot, A. Štrkalj, N. Pernet, J. L. Lado, C. Dorow, A. Lemaître, L. L. Gratiet, A. Harouri, I. Sagnes, S. Ravets, A. Amo, J. Bloch, and O. Zilberberg, Emergence of criticality through a cascade of delocalization transitions in quasiperiodic chains, *Nat. Phys.* **16**, 832 (2020).
  - [6] S. Roy, S. Chattopadhyay, T. Mishra, and S. Basu, Critical analysis of the reentrant localization transition in a one-dimensional dimerized quasiperiodic lattice, *Phys. Rev. B* **105**, 214203 (2022).
  - [7] U. Agrawal, R. Vasseur, and S. Gopalakrishnan, Quasiperiodic many-body localization transition in dimension  $d > 1$ , *Phys. Rev. B* **106**, 094206 (2022).
  - [8] X.-C. Zhou, Y.-J. Wang, T.-F. J. Poon, Q. Zhou, and X.-J. Liu, Exact New Mobility Edges between Critical and Localized States, *Phys. Rev. Lett.* **131**, 176401 (2023).
  - [9] S. Aubry and G. Andre, Analyticity breaking and Anderson localization in incommensurate lattices, *Ann. Israel Phys. Soc.* **3**, 133 (1980).

- [10] J. Biddle, D. J. Priour, B. Wang, and S. Das Sarma, Localization in one-dimensional lattices with non-nearestneighbor hopping: Generalized anderson and Aubry-André models, *Phys. Rev. B* **83**, 075105 (2011).
- [11] S. Xu, X. Li, Y.-T. Hsu, B. Swingle, and S. Das Sarma, Butterfly effect in interacting Aubry-André model: Thermalization, slow scrambling, and many-body localization, *Phys. Rev. Research* **1**, 032039 (2019).
- [12] T. Lv, Y.-B. Liu, T.-C. Yi, L. Li, M. Liu, and W.-L. You, Exploring unconventional quantum criticality in the  $p$ -wave-paired Aubry-André-Harper model, *Phys. Rev. B* **106**, 144205 (2022).
- [13] X. Bu, L.-J. Zhai, and S. Yin, Quantum criticality in the disordered Aubry-André model, *Phys. Rev. B* **106**, 214208 (2022).
- [14] X. Bu, L.-J. Zhai, and S. Yin, Kibble-zurek scaling in one-dimensional localization transitions, *Phys. Rev. A* **108**, 023312 (2023).
- [15] S. Ganeshan, J. H. Pixley, and S. Das Sarma, Nearest neighbor tight binding models with an exact mobility edge in one dimension, *Phys. Rev. Lett.* **114**, 146601 (2015).
- [16] A. Štrkalj, E. V. H. Doggen, I. V. Gornyi, and O. Zeitler, Many-body localization in the interpolating Aubry-André-Fibonacci model, *Phys. Rev. Research* **3**, 033257 (2021).
- [17] A. Purkayastha, S. Sanyal, A. Dhar, and M. Kulkarni, Anomalous transport in the Aubry-André-Harper model in isolated and open systems, *Phys. Rev. B* **97**, 174206 (2018).
- [18] J. Sutrardhar, S. Mukerjee, R. Pandit, and S. Banerjee, Transport, multifractality, and the breakdown of single-parameter scaling at the localization transition in quasiperiodic systems, *Phys. Rev. B* **99**, 224204 (2019).
- [19] V. Khemani, D. N. Sheng, and D. A. Huse, Two universality classes for the many-body localization transition, *Phys. Rev. Lett.* **119**, 075702 (2017).
- [20] H. Yao, A. Khoufli, L. Bresque, and L. Sanchez-Palencia, Critical behavior and fractality in shallow one-dimensional quasiperiodic potentials, *Phys. Rev. Lett.* **123**, 070405 (2019).
- [21] C. Yang, Y. Wang, P. Wang, X. Gao, and S. Chen, Dynamical signature of localization-delocalization transition in a one-dimensional incommensurate lattice, *Phys. Rev. B* **95**, 184201 (2017).
- [22] G. Roati, C. D'Errico, L. Fallani, M. Fattori, C. Fort, M. Zaccanti, G. Modugno, M. Modugno, and M. Inguscio, Anderson localization of a non-interacting Bose-Einstein condensate, *Nature* **453**, 895 (2008).
- [23] J. Billy, V. Josse, Z. Zuo, A. Bernard, B. Hambrecht, P. Lugan, D. Clément, L. Sanchez-Palencia, P. Bouyer, and A. Aspect, Direct observation of anderson localization of matter waves in a controlled disorder, *Nature* **453**, 891 (2008).
- [24] J. Biddle and S. Das Sarma, Predicted mobility edges in one-dimensional incommensurate optical lattices: An exactly solvable model of anderson localization, *Phys. Rev. Lett.* **104**, 070601 (2010).
- [25] A. Sinha, M. M. Rams, and J. Dziarmaga, Kibble-zurek mechanism with a single particle: Dynamics of the localization-delocalization transition in the Aubry-André model, *Phys. Rev. B* **99**, 094203 (2019).
- [26] B.-B. Wei, Fidelity susceptibility in one-dimensional disordered lattice models, *Phys. Rev. A* **99**, 042117 (2019).
- [27] J. C. C. Cestari, A. Foerster, M. A. Gusmano, and M. Continentino, Critical exponents of the disorder driven superfluid-insulator transition in one-dimensional Bose-Einstein condensates, *Phys. Rev. A* **84**, 055601 (2011).
- [28] X. Luo, T. Ohtsuki, and R. Shindou, Universality classes of the anderson transitions driven by non-hermitian disorder, *Phys. Rev. Lett.* **126**, 090402 (2021).
- [29] Y. Prasad and A. Garg, Single-particle excitations across the localization and many-body localization transition in quasiperiodic systems, *Phys. Rev. B* **109**, 094204 (2024).
- [30] S.-X. Zhang and H. Yao, Universal properties of many-body localization transitions in quasiperiodic systems, *Phys. Rev. Lett.* **121**, 206601 (2018).
- [31] R. Hamazaki, K. Kawabata, and M. Ueda, Non-Hermitian many-body localization, *Phys. Rev. Lett.* **123**, 090603 (2019).
- [32] L.-J. Zhai, S. Yin, and G.-Y. Huang, Many-body localization in a non-hermitian quasiperiodic system, *Phys. Rev. B* **102**, 064206 (2020).
- [33] A. Mostafazadeh, Pseudo-Hermiticity versus  $\mathcal{PT}$  symmetry: The necessary condition for the reality of the spectrum of a non-Hermitian Hamiltonian, *J. Math. Phys.* **43**, 205 (2001).
- [34] R. El-Ganainy, K. G. Makris, M. Khajavikhan, Z. H. Musslimani, S. Rotter, and D. N. Christodoulides, Non-Hermitian physics and  $\mathcal{PT}$  symmetry, *Nat. Phys.* **14**, 11 (2018).
- [35] Y. Ashida, Z. Gong, and M. Ueda, Non-Hermitian physics, *Adv. Phys.* **69**, 249 (2021).
- [36] M.-A. Miri and A. Al, Exceptional points in optics and photonics, *Science* **363**, eaar7709 (2019).
- [37] F. K. Kunst, E. Edvardsson, J. C. Budich, and E. J. Bergholtz, Biorthogonal bulk-boundary correspondence in non-Hermitian systems, *Phys. Rev. Lett.* **121**, 026808 (2018).
- [38] N. Okuma and M. Sato, Non-Hermitian topological phenomena: A review, *Ann. Rev. Cond. Matt. Phys.* **14**, 83 (2023).
- [39] X. Zhang, T. Zhang, M.-H. Lu and Y.-F. Chen, A review on non-Hermitian skin effect, *Adv. Phys.: X* **7**, 2109431 (2022).
- [40] K. Kawabata, K. Shiozaki, M. Ueda, and M. Sato, Symmetry and topology in non-Hermitian physics, *Phys. Rev. X* **9**, 041015 (2019).
- [41] D. S. Borgnia, A. J. Kruchkov, and R.-J. Slager, Non-Hermitian boundary modes and topology, *Phys. Rev. Lett.* **124**, 056802 (2020).
- [42] A. Li, H. Wei, M. Cotrufo, W. Chen, S. Mann, X. Ni, B. Xu, J. Chen, J. Wang, S. Fan, C.-W. Qiu, A. Al, and L. Chen, Exceptional points and non-Hermitian photonics at the nanoscale, *Nat. Nanotechnol.* **18**, 706 (2023).
- [43] S. Yao and Z. Wang, Edge states and topological invariants of non-hermitian systems, *Phys. Rev. Lett.* **121**, 086803 (2018).
- [44] S. Yao, F. Song, and Z. Wang, Non-Hermitian chern bands, *Phys. Rev. Lett.* **121**, 136802 (2018).
- [45] C.-X. Guo, C.-H. Liu, X.-M. Zhao, Y. Liu, and S. Chen, Exact solution of non-Hermitian systems with generalized boundary conditions: Sizedependent boundary effect and fragility of the skin effect, *Phys. Rev. Lett.* **127**, 116801 (2021).
- [46] N. Hatano and D. R. Nelson, Localization transitions in non-Hermitian quantum mechanics, *Phys. Rev. Lett.* **77**, 570 (1996).



- [47] N. Hatano and D. R. Nelson, Non-Hermitian delocalization and eigenfunctions, *Phys. Rev. B* **58**, 8384 (1998).
- [48] J.-Q. Cheng, S. Yin, and D.-X. Yao, Dynamical localization transition in the non-Hermitian lattice gauge theory, *Commun. Phys.* **7**, 58 (2024).
- [49] C. Wang and X. R. Wang, Anderson localization transitions in disordered non-hermitian systems with exceptional points, *Phys. Rev. B* **107**, 024202 (2023).
- [50] X.-W. Luo and C. Zhang, Photonic topological insulators induced by non-Hermitian disorders in a coupled-cavity array, *Appl. Phys. Lett.* **123**, 081111 (2023).
- [51] A. F. Tzortzakakis, K. G. Makris, and E. N. Economou, Non-Hermitian disorder in two-dimensional optical lattices, *Phys. Rev. B* **101**, 014202 (2020).
- [52] Z.-Q. Zhang, H. Liu, H. Liu, H. Jiang, and X. Xie, Bulk-boundary correspondence in disordered non-Hermitian systems, *Sci. Bull.* **68**, 157 (2023).
- [53] D.-W. Zhang, L.-Z. Tang, L.-J. Lang, H. Yan, and S.-L. Zhu, Non-hermitian topological Anderson insulators, *Sci. China Phys. Mech. Astron.* **63**, 267062 (2020).
- [54] S. Longhi, Topological phase transition in non-Hermitian quasicrystals, *Phys. Rev. Lett.* **122**, 237601 (2019).
- [55] S. Longhi, Metal-insulator phase transition in a non-Hermitian Aubry-Andrè-Harper model, *Phys. Rev. B* **100**, 125157 (2019).
- [56] X. Cai, Localization and topological phase transitions in non-hermitian Aubry-Andrè-Harper models with  $p$ -wave pairing, *Phys. Rev. B* **103**, 214202 (2021).
- [57] H. Jiang, L.-J. Lang, C. Yang, S.-L. Zhu, and S. Chen, Interplay of non-hermitian skin effects and Anderson localization in nonreciprocal quasiperiodic lattices, *Phys. Rev. B* **100**, 054301 (2019).
- [58] Y. Liu, Y. Wang, X.-J. Liu, Q. Zhou, and S. Chen, Exact mobility edges,  $pt$ -symmetry breaking, and skin effect in one-dimensional nonhermitian quasicrystals, *Phys. Rev. B* **103**, 014203 (2021).
- [59] T. Liu, H. Guo, Y. Pu, and S. Longhi, Generalized Aubry-Andrè self-duality and mobility edges in non-Hermitian quasiperiodic lattices, *Phys. Rev. B* **102**, 024205 (2020).
- [60] W. Chen, S. Cheng, J. Lin, R. Asgari, and X. Gao, Breakdown of the correspondence between the real-complex and delocalization-localization transitions in non-Hermitian quasicrystals, *Phys. Rev. B* **106**, 144208 (2022).
- [61] Z.-H. Wang, F. Xu, L. Li, D.-H. Xu, and B. Wang, Topological superconductors and exact mobility edges in non-Hermitian quasicrystals, *Phys. Rev. B* **105**, 024514 (2022).
- [62] S. Longhi, Non-Hermitian maryland model, *Phys. Rev. B* **103**, 224206 (2021).
- [63] A. Jazaeri and I. I. Satija, Localization transition in incommensurate non-Hermitian systems, *Phys. Rev. E* **63**, 036222 (2001).
- [64] P. Wang, L. Jin, and Z. Song, Non-Hermitian phase transition and eigenstate localization induced by asymmetric coupling, *Phys. Rev. A* **99**, 062112 (2019).
- [65] L.-J. Zhai, G.-Y. Huang, and S. Yin, Cascade of the delocalization transition in a non-Hermitian interpolating Aubry-Andrè-Fibonacci chain, *Phys. Rev. B* **104**, 014202 (2021).
- [66] L.-J. Zhai, G.-Y. Huang, and S. Yin, Nonequilibrium dynamics of the localization-delocalization transition in the non-Hermitian Aubry-Andrè model, *Phys. Rev. B* **106**, 014204 (2022).
- [67] L.-Z. Tang, G.-Q. Zhang, L.-F. Zhang, and D.-W. Zhang, Localization and topological transitions in non-Hermitian quasiperiodic lattices, *Phys. Rev. A* **103**, 033325 (2021).
- [68] C. Wu, J. Fan, G. Chen, and S. Jia, Non-Hermiticity-induced reentrant localization in a quasiperiodic lattice, *New J. Phys.* **23**, 123048 (2021).
- [69] C.-C. Zeng, Z. Cai, G.-H. Wang, and G. Sun, Fidelity and criticality in the nonreciprocal Aubry-Andrè-Harper model, arXiv:2404.16704 (2024).
- [70] V. M. Martinez Alvarez, J. E. Barrios Vargas, L. E. F. Foa Torres, Non-Hermitian robust edge states in one dimension: Anomalous localization and eigenspace condensation at exceptional points, *Phys. Rev. B* **97**, 121401(R) (2018).
- [71] S.-X. Zhang and H. Yao, Strong and weak many-body localizations, arXiv: 1906.00971 (2019).
- [72] L.-J. Zhai, L.-L. Hou, Q. Gao, and H.-Y. Wang, Kibble-Zurek scaling of the dynamical localization-skin effect phase transition in a non-Hermitian quasi-periodic system under the open boundary condition, *Front. Phys.* **10**, 1098551 (2022).
- [73] J. Bauer, T. M. Chang, and J. L. Skinner, Correlation length and inverse-participation-ratio exponents and multifractal structure for anderson localization, *Phys. Rev. B* **42**, 8121 (1990).
- [74] Y. V. Fyodorov and A. D. Mirlin, Analytical derivation of the scaling law for the inverse participation ratio in quasi-one-dimensional disordered systems, *Phys. Rev. Lett.* **69**, 1093 (1992).
- [75] E.-W. Liang, L.-Z. Tang, and D.-W. Zhang, Quantum criticality and kibble-zurek scaling in the Aubry-Andrè-Stark model, arXiv: 2405.10199 (2024).
- [76] S. Yin, G.-Y. Huang, C.-Y. Lo, and P. Chen, Kibble-Zurek scaling in the Yang-Lee edge singularity, *Phys. Rev. Lett.* **118**, 065701 (2017).
- [77] L.-J. Zhai, H.-Y. Wang, and S. Yin, Hybridized Kibble-Zurek scaling in the driven critical dynamics across an overlapping critical region, *Phys. Rev. B* **97**, 134108 (2018).
- [78] S. Hesselmann and S. Wessel, Thermal ising transitions in the vicinity of two-dimensional quantum critical points, *Phys. Rev. B* **93**, 155157 (2016).
- [79] M. A. Stephanov, Dimensional reduction and quantum-to-classical reduction at high temperatures, *Phys. Rev. D* **52**, 3746 (1995).
- [80] Z. Xu and S. Chen, Dynamical evolution in a one-dimensional incommensurate lattice with  $\mathcal{PT}$  symmetry, *Phys. Rev. A* **103**, 043325 (2021).
- [81] X. Cai, Boundary-dependent self-dualities, winding numbers, and asymmetrical localization in non-Hermitian aperiodic one-dimensional models, *Phys. Rev. B* **103**, 014201 (2021).